

Helicity transport in a simulated coronal mass ejection

B. Kliem^{1,2,3}, S. Rust¹ and N. Seehafer¹

¹Institute of Physics and Astronomy, University of Potsdam, Karl-Liebknecht-Str. 24-25,
14476 Potsdam, Germany

²Mullard Space Science Laboratory, University College London, Holmbury St. Mary, Dorking,
Surrey, RH5 6NT, UK

³Space Science Division, Naval Research Laboratory, Washington, DC 20375, USA

Abstract. It has been suggested that coronal mass ejections (CMEs) remove the magnetic helicity of their coronal source region from the Sun. Such removal is often regarded to be necessary due to the hemispheric sign preference of the helicity, which inhibits a simple annihilation by reconnection between volumes of opposite chirality. Here we monitor the relative magnetic helicity contained in the coronal volume of a simulated flux rope CME, as well as the upward flux of relative helicity through horizontal planes in the simulation box. The unstable and erupting flux rope carries away only a minor part of the initial relative helicity; the major part remains in the volume. This is a consequence of the requirement that the current through an expanding loop must decrease if the magnetic energy of the configuration is to decrease as the loop rises, to provide the kinetic energy of the CME.

Keywords. magnetic fields, (magnetohydrodynamics:) MHD, Sun: coronal mass ejections

1. Introduction

The helicity of the solar magnetic field obeys a hemispheric preference which is invariant with respect to the sign reversal of the global magnetic field with the activity cycle (Hale 1925; Seehafer 1990). This has led to the suggestion that coronal mass ejections (CMEs) must remove magnetic helicity from the Sun to prevent indefinite accumulation of the helicity in each hemisphere (Rust 1994; Low 1996). It was also found that the accumulation and removal of helicity can control the rate of mean-field dynamo action, so that the evolution of the activity cycle may be related to the flow of helicity through the Sun (Blackman & Field 2001; Brandenburg & Subramanian 2005). Careful studies of the long-term helicity budget of two solar active regions (Démoulin et al. 2002; Green et al. 2002) appear to confirm the conjecture of efficient helicity shedding by CMEs. However, both investigations used the linear force-free field approximation to estimate the helicity in the active region atmosphere. The accuracy of this estimate is not known. Similarly, the estimates of the helicity in interplanetary CMEs are still subject to considerable uncertainty (Démoulin 2007). In this paper, numerical simulation is used to quantify the transport of magnetic helicity from the source volume of CMEs.

2. Relative magnetic helicity in a simulated CME

We monitor the relative magnetic helicity $H_r = \int (\mathbf{A} + \mathbf{A}_p) \cdot (\mathbf{B} - \mathbf{B}_p) dV$ (Berger & Field 1984; Finn & Antonsen 1985) in an MHD simulation of a flux rope CME. The force-free equilibrium of a toroidal current channel partially submerged below the photosphere (Titov & Démoulin 1999) is chosen as initial condition. The twist is set to a supercritical

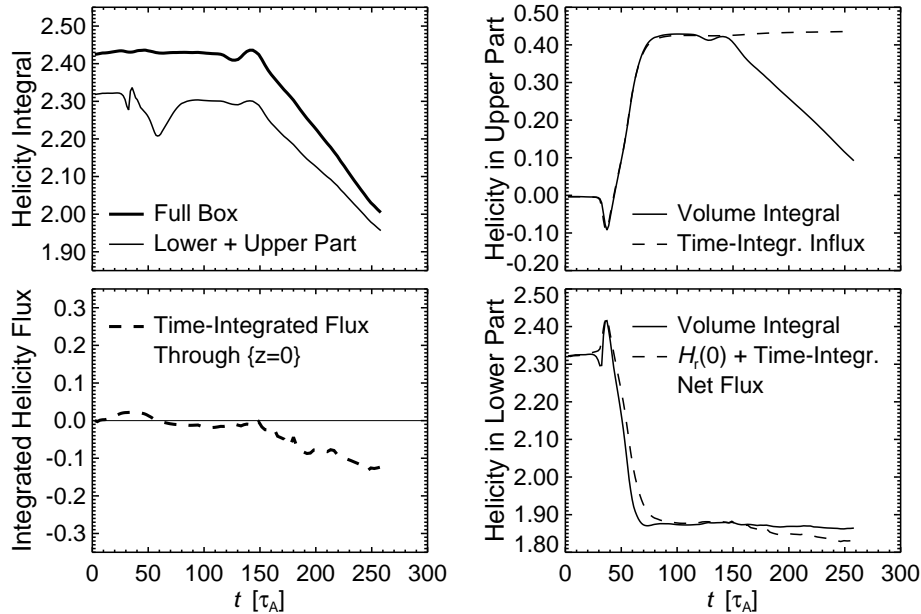


Figure 1. Relative magnetic helicity $H_r(t)$ in the simulation box and in the lower and upper sub-volumes, and time-integrated helicity fluxes through the bottom and diagnostics planes (bottom right) and through the diagnostics plane only (top right) in a CME simulation. The erupting flux begins to cross the diagnostics plane and the upper boundary of the box at $t \approx 30\tau_A$ and $t \approx 120\tau_A$, respectively. A helicity of about 0.4 (in normalized units) is transported from the lower into the upper sub-volume and then out of the box. This is about 1/5 of the initial helicity $H_r(0) \approx 2.4$. (The minor outflux of helicity through the bottom boundary for $t \gtrsim 150\tau_A$ results from downward propagating perturbations triggered by the ejected flux at large heights and may be a numerical artefact. The simulation was terminated by numerical instability in one of the upper corners of the box, where an open and two closed boundaries meet and numerical stability is more difficult to maintain than in the interior of the box.)

value, so that the kink-unstable magnetic flux rope formed by the current channel spontaneously starts to rise. The ideal MHD equations are integrated, neglecting pressure, with numerical diffusion enabling magnetic reconnection. The simulation is similar to the one in Török & Kliem (2005), except for an open upper boundary and a larger box size (of 40^3 unit lengths, set to be the initial flux rope apex height h_0). Approximations of the instantaneous helicity in the simulation box and of the helicity flux through the bottom boundary are obtained from Equations (1)–(7) in DeVore (2000). These are exact only if the field strength has fallen to zero at the top and lateral boundaries of the considered volume. We have checked that the computed approximate helicity of the initial equilibrium approaches a limit for increasing box size and that it deviates by less than 2% from the apparent limit value for the chosen size.

The approximation degrades as the flux rope passes through the top boundary, although the field strength then still decreases by more than two orders of magnitude from the bottom to the top of the box. To estimate the magnitude of the error, we divide the box by a horizontal “diagnostics plane” at height $z = 6h_0$, such that the field drops with increasing height by a similar factor in each sub-volume. At $t = 0$ the factor is of order 10^2 , justifying the use of the approximation in each sub-volume. The top left panel in Figure 1 shows that the summed helicities of the sub-volumes differ by $\lesssim 5\%$ from the helicity of the box as a whole, with the error obviously originating from the lower sub-volume, since $H_r(t=0) = 0$ is correctly found in the upper sub-volume (top right

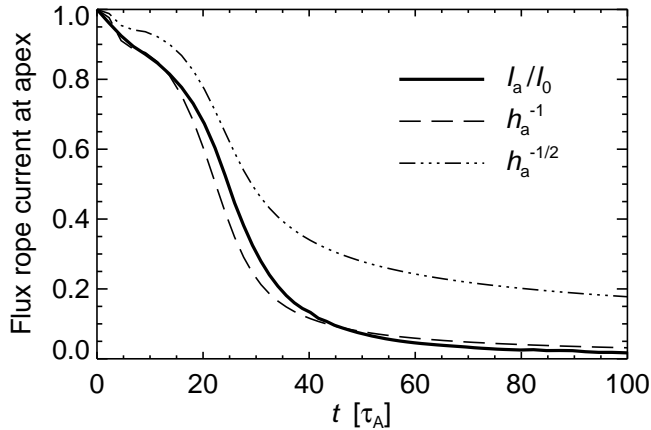


Figure 2. Total current through the apex of the flux rope, normalized by initial current, $I_a(t)/I_0$. For comparison, the inverse of the apex height $h_a(t)$, a proxy for the flux rope length, and $h_a(t)^{-1/2}$ are shown (see text).

panel). When the upper part of the unstable flux rope begins to propagate through the diagnostics plane, the approximation is degraded in the lower sub-volume, but is still of similar quality as before in the upper sub-volume and in the box as a whole. The resulting error is given by the additional difference between the two values for the whole volume in the relevant time interval, $t \sim (30-80)\tau_A$, where $\tau_A = h_0/V_A$ and V_A is the initial Alfvén velocity in the flux rope. The error reaches a peak value $\lesssim 5\%$ at $t = 60\tau_A$, when the flux rope apex has risen to $z = 17h_0$, and decreases considerably thereafter. The helicity calculation for $t \gtrsim 120\tau_A$, when the CME leaves the box, should even be more precise, since the field strengths of the flux rope at the upper boundary are then smaller, by an order of magnitude, than the field strengths at the passage of the diagnostics plane.

Figure 1 shows that a relative helicity of ≈ 0.4 (in the normalized units of the simulation, which prescribe a field strength of unity at the apex of the initial flux rope, $|\mathbf{B}_0(0, 0, 1)| = 1$) is transported from the lower into the upper subvolume and then out of the box when the upper part of the erupting flux rope crosses the respective top boundary. (A helicity of ≈ 0.1 is not yet ejected when the simulation is terminated due to numerical instability, but it is clear from the plot that this will be ejected as well.) The top right plot shows a very small rate of helicity flux through the diagnostics plane after the top part of the flux rope has propagated into the upper sub-volume ($t \gtrsim 80\tau_A$). This suggests that the further upward stretching of the flux rope legs and the addition of flux to the rope by reconnection in the vertical current sheet under the rope do not contribute strongly to the ejected helicity, at least not at the scales covered by the simulation, which extend to flux rope apex heights of ≈ 25 times the footpoint distance (several solar radii when scaled to a large solar active region). The upward reconnection outflow velocity, a proxy of the reconnection rate in our ideal MHD simulation, has decreased to one quarter of its peak value, $u_z(t = 52) = 0.8V_A$, by the end of the simulation. The soft X-ray flux of long-duration solar ejective events, an indicator of the energy release by reconnection, decreases strongly from its peak value on such scales. Therefore, although this simulation is terminated by numerical instability, it likely models most of the helicity ejection in a CME. However, this amounts to only about $1/5$ of the initial relative helicity.

The relatively small efficiency of helicity ejection can be related to the evolution of the current distribution in the volume. These currents carry the relative helicity (which vanishes in a potential field). The initial coronal equilibrium consists of a section of a toroidal

current ring. The energy of a current ring is given by $W = LI^2/2 \approx I^2 R [\ln(8R/a) - 7/4]$, where I , R , a , and L are the current, major and minor radius, and the inductance of the ring, respectively. Since magnetic energy must be released in order to accelerate the ejecta and the term in brackets does not vary strongly, the current in the rising flux loop of the CME must decrease faster than $R^{-1/2}$. In the approximation of ideal MHD the current in the loop decreases roughly as R^{-1} , because the number of field line turns in the loop is conserved. The simulation shows such a fast decrease (Figure 2), which results in most of the current staying low in the box. Consequently, only a minor part of the initial relative helicity leaves the system with the ejected flux.

3. Conclusions and Discussion

The simulated CME ejects only a minor part of the initial relative magnetic helicity from its source volume. Although this result requires substantiation through the study of its parametric dependence and of other equilibria, the necessary decrease of the current through an expanding unstable flux loop leads us to expect that it holds generally. The number of CMEs per active region varies within very wide limits. Between 30 and 65 CMEs have been estimated to occur throughout the lifetime of the two very CME-prolific active regions studied in Démoulin et al. (2002) and Green et al. (2002). On the other hand, the majority of active regions produces no CME at all, or only one CME in their lifetime. Hence, the shedding of helicity by CMEs may be of lower importance than originally conjectured.

It appears natural to assume that, perhaps generally, much of an active region's helicity submerges when the region disperses and the major part of its flux submerges below the photosphere. The helicity may then follow the slow journey of magnetic flux in the course of the solar cycle. Annihilation of helicity in the interior of the Sun, following the transport of the helicity-carrying flux to the equatorial plane by the meridional flow, is one possibility to prevent the helicity in each hemisphere from accumulating indefinitely. Another possibility, opposite to a common conjecture, is that the helicity in the solar interior, like magnetic energy, undergoes a normal (or direct) turbulent cascade towards small spatial scales, where it is dissipated. Also, the cascade directions may be different for small-scale and large-scale fields (Alexakis et al. 2006), with the helicity of active-region magnetic fields, considered to be small-scale fields, subject to a direct cascade.

References

- Alexakis, A., Mininni, P. D., & Pouquet, A. 2006, *ApJ* 640, 335
 Berger, M. A., & Field, G. B. 1984, *J. Fluid Mechanics* 147, 133
 Blackman, E. G., & Field, G. B. 2001, *Phys. Plasmas* 8, 2407
 Brandenburg, A., & Subramanian, K. 2005, *Physics Reports* 417, 1
 Démoulin, P. 2007, *Adv. Space Res.* 39, 1674
 Démoulin, P., Mandrini, C. H., van Driel-Gesztelyi, L., et al. 2002, *A&A* 382, 650
 DeVore, C. R. 2000, *ApJ* 539, 944
 Finn, J. M., & Antonsen, T. M. 1985, *Comm. Plasma Phys. Contr. Fusion* 9, 111
 Green, L. M., López Fuentes, M. C., Mandrini, C. H., et al. 2002, *Solar Phys.* 208, 43
 Hale, G. E. 1925, *Publ. Astron. Soc. Pacific* 37, 268
 Low, B.-C. 1996, *Solar Phys.* 167, 217
 Rust, D. M. 1994, *Geophys. Res. Lett.* 21, 241
 Seehafer, N. 1990, *Solar Phys.* 125, 219
 Titov, V. S., & Démoulin, P. 1999, *A&A* 351, 707
 Török, T., & Kliem, B. 2005, *ApJ* 630, L97